HAL
open science

Effect of build orientation on the manufacturing process and the properties of stereolithographic dental ceramics for crown frameworks

Marion Dehurtevent, Lieven Robberecht, Anthony Thuault, Etienne Deveaux, Anne Leriche, Fabrice G. Petit, Corentin Denis, Jean-Christophe Hornez, Pascal Béhin

To cite this version:

Marion Dehurtevent, Lieven Robberecht, Anthony Thuault, Etienne Deveaux, Anne Leriche, et al.. Effect of build orientation on the manufacturing process and the properties of stereolithographic dental ceramics for crown frameworks. Journal of Prosthetic Dentistry, 2021, 125 (3), pp.453-461. 10.1016/j.prosdent.2020.01.024 . hal-03479576

HAL Id: hal-03479576

https://uphf.hal.science/hal-03479576v1

Submitted on 10 Mar 2023

HAL is a multi-disciplinary open access archive for the deposit and dissemination of scientific research documents, whether they are published or not. The documents may come from teaching and research institutions in France or abroad, or from public or private research centers.

L'archive ouverte pluridisciplinaire **HAL**, est destinée au dépôt et à la diffusion de documents scientifiques de niveau recherche, publiés ou non, émanant des établissements d'enseignement et de recherche français ou étrangers, des laboratoires publics ou privés.

Distributed under a Creative Commons Attribution - NonCommercial 4.0 International License

Version of Record: https://www.sciencedirect.com/science/article/pii/S0022391320300925
Manuscript_172f2bcacfe555b57c5cbbfaf8f33c68

Effect of build orientation on the manufacturing process and the properties of stereolithographic dental ceramics for crown frameworks

Marion Dehurtevent, DDS, PhD,[a] Lieven Robberecht, DDS, PhD,[b] Anthony Thuault, PhD,[c] Etienne Deveaux, DDS, PhD,[d] Anne Leriche, PhD,[e] Fabrice Petit, PhD,[f] Corentin Denis, DDS,[g] Jean-Christophe Hornez, PhD,[h] and Pascal Béhin, DDS, PhD[i]

[a]Associate Professor, Department of Prosthodontics, Faculty of Dental Surgery, University of Lille, Lille, France.

[b]Associate Professor, Department of Restorative Dentistry, Faculty of Dental Surgery, University of Lille, Lille, France.

[c]Associate Professor, Laboratory of Ceramic Materials and Associated Processes, Université de Valenciennes, Maubeuge, France.

[d]Professor, Department of Restorative Dentistry, Faculty of Dental Surgery, University of Lille, Lille, France.

[e]Professor, Laboratory of Ceramic Materials and Associated Processes, Université Polytechnique des Hauts de France, Maubeuge, France.

[f]Associate Professor, Belgian Ceramic Research Centre, Mons, Belgium.

[g]Associate Professor, Department of Prosthodontics, Faculty of Dental Surgery, University of Lille, Lille, France.

[h]Associate Professor, Laboratory of Ceramic Materials and Associated Processes, Université de Valenciennes, Maubeuge, France.

© 2020 published by Elsevier. This manuscript is made available under the CC BY NC user license
https://creativecommons.org/licenses/by-nc/4.0/

[i]Professor, Department of Prosthodontics, Faculty of Dental Surgery, University of Lille, Lille, France.

*MD and LR contributed equally in this work.

Corresponding author

Dr Marion Dehurtevent

Department of Prosthodontics

Faculty of Dentistry

University of Lille

FRANCE

Email: marion.dehurtevent@univ-lille.fr

JPD-19-806

RESEARCH AND EDUCATION

Effect of build orientation on the manufacturing process and the properties of stereolithographic dental ceramics for crown frameworks

Marion Dehurtevent, DDS, PhD,[a] Lieven Robberecht, DDS, PhD,[b] Anthony Thuault, PhD,[c] Etienne Deveaux, DDS, PhD,[d] Anne Leriche, PhD,[e] Fabrice Petit, PhD,[f] Corentin Denis, DDS,[g] Jean-Christophe Hornez, PhD,[h] and Pascal Béhin, DDS, PhD[i]

[a]Associate Professor, Department of Prosthodontics, Faculty of Dental Surgery, University of Lille, Lille, France.

[b]Associate Professor, Department of Restorative Dentistry, Faculty of Dental Surgery, University of Lille, Lille, France.

[c]Associate Professor, Laboratory of Ceramic Materials and Associated Processes, Université de Valenciennes, Maubeuge, France.

[d]Professor, Department of Restorative Dentistry, Faculty of Dental Surgery, University of Lille, Lille, France.

[e]Professor, Laboratory of Ceramic Materials and Associated Processes, Université Polytechnique des Hauts de France, Maubeuge, France.

[f]Associate Professor, Belgian Ceramic Research Centre, Mons, Belgium.

[g]Associate Professor, Department of Prosthodontics, Faculty of Dental Surgery, University of Lille, Lille, France.

[h]Associate Professor, Laboratory of Ceramic Materials and Associated Processes, Université de Valenciennes, Maubeuge, France.

[i]Professor, Department of Prosthodontics, Faculty of Dental Surgery, University of Lille, Lille, France.

*MD and LR contributed equally in this work.

ABSTRACT

Statement of problem. Stereolithographic (SLA) ceramic crown frameworks are suitable for clinical use, but the impact of SLA build orientation has not been identified.

Purpose. The purpose of this in vitro study was to investigate the effect of 3 build orientations on the physical and mechanical properties and the microstructure of SLA alumina dental ceramics.

Material and methods. The physical and mechanical properties and microstructures of 3 different oriented SLA alumina ceramics (ZX, ZY, and XY) were evaluated by visual observation, hydrostatic weighing (n=10/group), Weibull analyses (n=30/group), scanning electron microscopy, 3-point flexural strength (n=30/group), fracture toughness (indentation, single-edge-V-notched-beam) (n=4/group), and Vickers hardness (n=15/group) testing. The hydrostatic weighing, 3-point flexural strength, fracture toughness, and Vickers hardness testing data were statistically analyzed (α=.05).

Results. The minimum resting period of slurries between the polymerization of 2 layers was shorter for the ZY- and ZX-oriented specimens and increased with the layer surface. The density and Vickers hardness of the SLA-manufactured specimens were similar for all groups (P>.05). The 95% confidence intervals of the Weibull moduli of the ZX- and ZY-oriented specimens

were higher than that of the XY-oriented specimens, with no overlap fraction. The ZY-oriented specimens displayed significantly higher 3-point flexural strength ($P<.05$) and fracture toughness as evaluated by the single-edge-V-notched-beam method than the ZX-oriented specimens ($P<.05$). They also displayed significantly higher 3-point flexural strength than the XY-oriented specimens ($P<.05$). The microstructural analysis showed that the texturing was heterogeneous and that the major axis of the large grains of alumina ran parallel to the orientation of the layers. **Conclusions.** The ZY-orientation produced a reliable dental ceramic by SLA, with the shortest general manufacturing time and the highest mechanical strength when the layers were perpendicular to the test load surface.

CLINICAL IMPLICATIONS.

SLA dental ceramics fabricated with the layers perpendicular to the occlusal surface had the best properties. This will help technicians fabricate suitable and reliable SLA crown frameworks.

INTRODUCTION

Additive manufacturing is a technology that builds 3D objects by adding material in layers. This method is being used to manufacture metal and polymer objects for dental use but is still in the early stages of development for shaping dental ceramics.[1-6] Additive manufacturing is an effective way to avoid the major drawbacks associated with subtractive manufacturing, which involves shaping a solid block of material, including waste of raw material, wear of milling tools, shape limitations, and microscopic cracks that can weaken restorations.[7] Stereolithography (SLA) is an additive manufacturing process that produces objects in a layer-by-layer fashion using a photosensitive resin. The monomers are polymerized to form the body of a 3D solid. The

monomers can also be mixed with ceramic particles to form a photosensitive slurry for producing ceramic objects. SLA shows more promise than other additive manufacturing methods because it can be used to build crown frameworks that meet dental standards (ISO 6872:2015).[8] SLA involves designing 3D objects supported by pillars, slicing, transferring to SLA software and equipment, layer-by-layer polymerization of a ceramic slurry containing a photosensitive resin, hand sectioning of the pillars, thermal debinding, and sintering. A complex object can be manufactured with different build orientations, which has an impact on the size of the different layers.[6] To avoid deformations of the object during the manufacturing process, a minimum slurry resting period must be adopted immediately after the polymerization of a layer.

SLA alumina ceramic crown frameworks with high density, flexural strength, and Weibull modulus values can be built and are suitable for clinical use.[6] A smaller slurry organic phase also results in fewer defects in SLA alumina ceramics, and an 80% (w/w) slurry dry matter content is the best compromise for the manufacturing process.[6] Despite the high mechanical strength, feasibility, and structural reliability of SLA objects, this approach remains controversial because of the anisotropic shrinkage of alumina ceramics that occurs during the densification step,[9] which could have a negative impact on the mechanical behavior of the ceramic. The orientation of ceramic particles has an effect on the mechanical behavior of ceramics as does the general build orientation on the mechanical properties of SLA resins.[10,11] This results in an anisotropic behavior of additive-manufactured materials.[12] This highlights the need to investigate the effect of this parameter on ceramics. Pfaffinger et al[13] investigated 2 build orientations for densified tricalcium phosphate ceramics and reported that slurry composition affected flexural strength in the build orientation. Dental restorations require high flexural strength, density, hardness, fracture toughness, and structural reliability to ensure

durability. Fracture toughness can be measured on the surface of a ceramic specimen by using the indentation technique but is influenced by the microstructure of the specimen.[14-16] The single-edge-V-notched-beam (SEVNB) method is a precise technique for measuring fracture toughness, but the microstructure of the ceramic may affect notch preparation, and precracks may underestimate the results.[17] The 2 methods are thus complementary.

Manufacturing time should be minimized, so the minimal resting period of the slurry between the polymerization of 2 layers must be determined with respect to the build orientation. These physical and mechanical properties must be studied in 3 orthogonal planes (ZX, ZY, and XY) of 3 build orientations in order to meet the ISO6872:2015[8] standard and to optimize the orientation of the SLA crown frameworks and obtain the best mechanical behavior for clinical use. This will make it possible to determine the optimal build orientation with respect to the main masticatory stresses of prostheses and their position in the dental arch, which will provide the best mechanical strength and reproducibility and the shortest manufacturing time (buccolingual, mesiodistal, or occlusocervical directions).

The purpose of this in vitro study was to evaluate the impact of 3 build orientations on the physical properties (minimum resting period between the polymerization of 2 layers, density), mechanical properties (3-point flexural strength, Weibull modulus, hardness, fracture toughness by indentation and by SEVNB), and microstructure of SLA alumina dental ceramics. The null hypotheses were that the build orientation would not affect the physical properties, the mechanical properties, or the microstructure of SLA alumina dental ceramics.

MATERIAL AND METHODS

Slurries were prepared using alumina powders (CT1200SG; Almatis). The powders were dried for 1 hour at 90 °C in an oven (Beschickung loading model 100-800; Memmert). The powders were incorporated into a photosensitive (λ=350-400 nm) acrylic resin (C1-alumina; CryoBeryl Software) to obtain 80% (w/w) dry matter content slurries that were homogenized at 150 rpm by planetary milling for 30 minutes (PM100; Retsch). The rectangular parallelepipedal specimens were designed using CAD software (Catia; Dassault Systèmes). Their dimensions were 1.3×4×22 mm for the evaluation of density, 3-point flexural strength, Weibull modulus, hardness, fracture toughness by indentation, and microstructure assays and 3×4×40 mm for the evaluation of fracture toughness by the SEVNB – 3-point bending test (Fig. 1A).

All the specimens were oriented in 3 different planes to ensure that their widths and lengths were situated within the ZX, ZY, and XY axes (Fig. 1B), making it possible to produce ZX-, ZY-, and XY-oriented specimens. The specimens were supported on pillars (end diameter: 0.2 mm, base diameter: 0.7 mm, height: 2 mm) during the design step. The models were oversized to compensate for the anisotropic shrinkage that occurs during the thermal treatment of SLA alumina.[6] The specimens were then sliced (layer thickness=50 µm) (Creation Workshop software; Datatree3D), and the data were transferred to SLA software (CryoCeram; CryoBeryl Software) and equipment (CryoCeram Printer; CryoBeryl Software) for additive manufacturing (polymerization energy=10 $mW.cm^{-2}$, resolution=50 µm).

The entire surface of a layer was polymerized at once using a dynamic mask of digital micromirror devices. The support platform was then moved down into the slurry. The pillars were hand sectioned after the manufacturing phase. The specimens were debinded (0.1 °C/minute, 450 °C, 2-hour dwell time) in an oven (LHT; Carbolite) and were sintered (15 °C/minute, 1690 °C, 3-hour dwell time) (HT16/17; Nabertherm).

Specimens (n=3/group) were prepared with different slurry resting periods (6, 7, 8, 9, 10, 11, and 12 seconds) before polymerizing a layer. The minimum slurry resting period between the polymerization of 2 layers was set as the time when no visual macroscopic deformations of the manufactured object were observed. The density of the specimens was determined by hydrostatic weighing using the Archimedes principle (3 vacuum cycles, n=10/group).

The 3-point flexural strength was determined using a universal testing machine (DY30; Adamel Lhomargy) (n=30/group) with a maximum force of 1 kN. Based on the ISO 6872:2015 standard,[8] a progressive central vertical load was applied at a speed of 0.5 mm/minute on the dark grey face of the specimens (Fig. 1B). The distance between the lower supports was 20 mm. The 3-point flexural strength in MPa (σ) was (equation 1): $\sigma - (3 \times F \times L)/(2 \times W \times H^2)$, where F is the maximum force to failure (N), L is the distance between the lower supports (mm), W is the specimen width (mm), and H is the specimen height (mm). A Weibull distribution analysis using 3-point flexural strength data was used to assess the structural reliability of the ceramics (n=30/group). The Weibull modulus (m) was $P_f = 1 - \exp[-(\sigma/\sigma_0)^m]$, where P_f is the probability of failure between 0 and 1, σ is the 3-point flexural strength in MPa, and σ_0 is the characteristic strength in MPa.

A Vickers indentation hardness test (ZHU 0.2, Zwick) was performed (ISO 14705:2016) (n=15/group).[18] A 2-N load was applied to force the indenter into the test piece and hold it in place for 13 seconds, and the diagonals (d) of the impression were measured. The Vickers hardness in Hv was $Hv = 0.1891.\ P/d^2$, where P is the load (N) and d is the impression diagonal (mm). The microhardness was evaluated on 3 faces: thickness-length, length-width, and width-thickness (n=15/face). Fracture toughness (K_{IC}) was determined by SEVNB – 3-point bending using a universal testing machine (Zwick Z100). A V-notch of uniform depth was created in all

the specimens by using a 0.3-mm cutoff wheel mounted on a cutting machine (Struers Discotom 100). The specimens were loaded using a 3-point bend fixture (30-mm outer span and 15-mm inner span) with a crosshead speed of 0.5 mm/minute (n = 4/group). Fracture toughness was $K_{IC} = F.S/B.W^{1.5}.3\sqrt{\alpha}/2.Y$, where α is the initial precrack relative length (m), W is the specimen width (m), B is the specimen thickness (m), F is the fracture load (MN), and S is the support span (m).

The indentation fracture toughness was determined using the indentation cracking method (ASTM STP 678).[19] Vickers indentations were impressed (F=20 N) (n=4/group). The crack lengths were measured on 3 faces using a scanning electron microscope. The fracture toughness by indentation in MPa.m$^{1/2}$ (K_1C) was $K_{IC} = 0{,}016.F/c^{3/2}.(E/Hv)^{1/2}$, where F is the indentation load (N), c is the average crack length (mm), E is the Young modulus (GPa), and Hv is the hardness (GPa).

The microstructures of the mirror-polished surfaces were observed by scanning electron microscopy (S-3500N; Hitachi) (magnification ×2000) on 3 faces (Fig. 1). Additionally, the fracture surfaces of the 3-point flexural strength specimens were observed by scanning electron microscopy (magnification ×25 and ×1500).

Specimen sizes were determined in order to reach a minimal statistical power of 95%. The normality of data distribution was verified using the Kolmogorov-Smirnov test. The density, microhardness, and fracture toughness values were analyzed by using the 1-way Kruskal-Wallis test and Dunn post hoc test. Three-point flexural strength was analyzed using a 1-way ANOVA test and the Tukey multiple comparison post hoc test (GraphPad 5; Prism) (α=.05).

RESULTS

The results of the physical and mechanical measurements are summarized in Table 1. Figure 2 shows box plots of these results. The minimum slurry resting period between the polymerization of 2 layers varied from 7 seconds to 11 seconds depending on the build orientation (Table 1). The minimum resting period was 11 seconds for the XY-oriented specimen, 8 seconds for the ZY-oriented specimen, and 7 seconds for the ZX-oriented specimen. The general manufacturing time was 35 minutes for the XY-oriented specimen, 47 minutes for the ZY-oriented specimen, and 3 hours 6 minutes for the ZX-oriented specimen. The densities of the SLA specimens were similar for all groups (P>.05) (Fig. 2, Table 1).

The 3-point flexural strength of the ZY-oriented specimens (409.7 ±29.6 MPa) was significantly higher than that of the ZX-oriented specimens (313.8 ±27.9 MPa and the XY-oriented specimens (334.3 ± 62.1 MPa) (P<.05) (Fig. 2, Table 1). The Weibull moduli of the ZX- oriented specimens (13.7 [12.4-15.1]) and the ZY-oriented specimens (16.1 [14.6-17.5]) were higher than that of the XY-oriented specimens (6.2 [5.6-6.8]) (Fig. 3, Table 1). No difference in hardness was found regardless of the face considered for all the groups (P>.05) (Fig. 2, Table 1). The fracture toughness of the ZY-oriented specimens (4.6 ±0.2 MPa.m^{½}) as determined by SEVNB was significantly higher than that of the ZX-oriented specimens (3.2 ±0.2 MPa.m^{½}) (P<.05). In contrast, the fracture toughness of all the faces as determined by indentation was similar for all the specimens (P>.05) (Fig. 2, Table 1).

All the specimens were microporous and displayed no signs of delamination. In addition, the major axis of the large grains of alumina was parallel to the orientation of the layers (Fig. 4). In terms of the fracture surface analysis, more transgranular failures were observed inside the

alumina particles with the ZY- and XY-oriented specimens than with the ZX-oriented specimens (Fig. 5), while more intergranular failures were observed with the ZX-oriented specimens.

DISCUSSION

The null hypotheses that the build orientation would have no impact on the physical properties, the mechanical properties, or the microstructure of SLA alumina dental ceramics were rejected. In general, the physical and mechanical properties and microstructure of SLA alumina ceramics were influenced by the orientation of the printed layers.

The ZX-oriented specimens had the smallest layer surface and required the shortest minimum resting period between the polymerization of 2 layers. The present study showed that the smaller the layer surface, the shorter the minimum resting period. However, the ZX orientation increased the number of layers and had a negative impact on the manufacturing time. The build orientation had an impact on the minimum resting period and the manufacturing time. Given this, a compromise that took the shortest minimum resting period of the slurry and the lowest number of layers into account had to be found. The XY-oriented specimens best met this requirement, with an 11-second minimum resting period for the slurry, 34 layers, and a general manufacturing time of 35 minutes. The ZY-oriented specimens (general manufacturing time: 50 minutes) were also a good compromise with respect to the ZX-oriented specimens (general manufacturing time: 3 hours). Although the XY-oriented specimens had the shortest general manufacturing time, their mechanical strength was lower.

In terms of the physical properties of densified SLA alumina ceramics, the density of the alumina ceramics was close to 98% after the thermal treatment and was similar for all the build orientations. It has been previously reported that high density results in fewer cracks and reduces

the delamination of SLA ceramics.[13,20] The densities of the ceramics used in the present study were thus acceptable for clinical use and were consistent with previous work on alumina and tricalcium phosphate.[6,13]

In terms of mechanical properties, the SLA specimens displayed anisotropic behavior. The 3-point flexural strengths of all the specimens were above 300 MPa and corresponded to the dental ISO6872:2015 standard[8] regardless of the build orientation. The ZY-oriented specimens had the highest 3-point flexural strength (409.7 ±29.6 MPa). More transgranular failures were observed in the ZY-oriented (perpendicular to the load surface) and XY-oriented specimens (perpendicular to the load direction) and more intergranular failures in the ZX-oriented specimens. Furthermore, the microstructural analysis revealed heterogeneous texturing, with the main axis of the large grains and the orientation of the layers parallel for all specimens.

The flexural strength results can be explained by previous studies, which showed that ceramic specimens with the load perpendicular to the grain axis display more transgranular failures, which results in a higher mechanical strength than when the load is parallel to the grain axis.[21,22] Further studies on the microstructural modifications that occur during the densification of ceramics will be required to better understand this texturing. However, this does not explain why the ZY-oriented specimens (perpendicular to the test load surface) displayed a higher 3-point flexural strength than the XY-oriented specimens (perpendicular to the direction of the test load), which also have a main axis of large grains perpendicular to the direction of the load. These results might, however, be explained by the morphological texturing and spatial orientation of the large grains, which should be investigated in future studies. The evaluation of the structural reliability of dental ceramics by the Weibull analysis provided additional answers to this issue. The Weibull moduli of the ZX- and ZY-oriented specimens were similar to those

reported in the literature.[23] The XY-oriented specimens had the lowest Weibull modulus, indicating that they have less structural reliability than the ZX- and ZY-oriented specimens.[23] Pfaffinger et al[13] suggested that low Weibull moduli can result from defects in SLA ceramics, which leads to anisotropic mechanical behavior. In the present study, the XY-oriented specimens had the greatest layer surface with the longest resting periods. This can increase the risk of defects within the layers and may explain the lower Weibull moduli observed in this group. To test this hypothesis, the maximum layer surface that does not reduce the Weibull moduli should be determined.

The hardness values followed the same trend as the density values. The hardness of the ceramic specimens was similar, regardless of the SLA orientation, suggesting that this parameter is isotropic in nature and only depends on grain size and relative density.[15] However, consistent with Uçar et al,[24] these values were higher than those of other alumina ceramics manufactured by subtractive methods for dental applications.[25] This could be explained by the textured aspect of SLA ceramics.[15,16]

The fracture toughness of the SLA ceramics depended on the evaluation method used. However, these results should be considered preliminary given the small sample size. Fracture toughness evaluated by indentation has been used for a first analysis of a new ceramic.[14] In the present study, fracture toughness evaluated by indentation followed the same trend as hardness. SEVNB is a more precise method for evaluating fracture toughness than indentation, a local measurement method.[15] This technique gave higher fracture toughness values for the ZY-oriented specimens than for the ZX-oriented specimens. Once again, this shows that the microstructure of SLA ceramics had an impact on their mechanical behavior, suggesting that the

heterogeneous texturing increased the fracture toughness as determined by the SEVNB method when the layer is perpendicular to the load surface.[10]

Transposed to a clinical context, these results showed that ZY- and ZX-oriented frameworks generate an orientation of the printed layers perpendicular to the occlusal surface and thus parallel to the direction of the main masticatory stresses applied to the occlusal surface (Fig. 6). In this situation, and with these experimental conditions, both oriented ceramics would have the best reproducibility. Furthermore, preference should be given to a short general manufacturing time (compromise between a small number of layers and a small layer surface). The ZY-orientation should thus be preferred because it has the shortest general manufacturing time and has layers that are parallel to the main direction of the masticatory stresses. For a complex crown framework shape, and if the Z axis is considered as the occlusocervical direction, the orientation of the layers that results in both the shortest manufacturing time and layers parallel to the direction of the masticatory stresses are the buccolingual direction for incisors and premolars and the mesiodistal or buccolingual directions for molars in terms of the anatomy of the crown (Fig. 7). However, a clinical extrapolation of these experimental results must be tempered, as the complexity of a crown shape represents both the ZY- and ZX-oriented experimental conditions. These results must be confirmed with future investigations that simulate the more complex masticatory stresses that ceramics and other materials such as zirconia are subjected to. The maximum layer surface of a complex crown framework must be determined in this way and other layer orientations should be investigated.[11]

CONCLUSIONS

Based on the findings of this in vitro study, the following conclusions were drawn:

1. All the SLA alumina ceramics studied met dental standards.
2. The orientations of the SLA ceramics in 3 orthogonal planes affected the minimum resting period of the slurry between the polymerization of 2 layers, as well as the physical and mechanical properties of the sintered objects ($P<.05$).
3. The minimum resting period of the slurry needed between the polymerization of 2 layers increased with the layer surface.
4. The ZY-oriented specimens with the smallest number of layers and a layer orientation perpendicular to the occlusal surface provided the best compromise between mechanical strength and general manufacturing time ($P<.05$).

REFERENCES

1. Antanasova M, Kocjan A, Hočevar M, Jevnikar P. Influence of surface airborne-particle abrasion and bonding agent application on porcelain bonding to titanium dental alloys fabricated by milling and by selective laser melting. J Prosthet Dent 2019 [Epub ahead of print].

2. Liu W, Qing H, Pei X, Wang J. Internal adaptation of cobalt-chromium posts fabricated by selective laser melting technology. J Prosthet Dent 2019;121:455-60.

3. van Noort R. The future of dental devices is digital. Dent Mater 2012;28:3-12.

4. Denry I, Kelly JR. Emerging ceramic-based materials for dentistry. J Dent Res 2014;93:1235-42.

5. Eckel ZC, Zhou C, Martin JH, Jacobsen AJ, Carter WB, Schaedler TA. Additive manufacturing of polymer-derived ceramics. Science 2016;351:58-62.

6. Dehurtevent M, Robberecht L, Deveaux E, Thuault A, Hornez JC, Béhin P. Stereolithography: a new method for processing dental ceramics by additive CAD/CAM. Dent Mater 2017;33:477-85.

7. Wang H, Aboushelib MN, Feilzer AJ. Strength influencing variables on CAD/CAM zirconia frameworks. Dent Mater 2008;24:633-8.

8. International Organization for Standardization. ISO 6872:2015. Dentistry – Ceramic materials. Geneva: International Organization for Standardization; 2015. AFNOR Store Order: N20200117-438973-T (Date: 2020-01-17). Available at: http://www.boutique.afnor.org.

9. Cawley JD. Solid freeform fabrication of ceramics. Curr Opin Solid State Mater Sci 1999;4:483-9.

10. Cesar PF, Della Bona A, Scherrer S, Tholey M, van Noort et al. ADM guidance–ceramics: fracture toughness testing and method selection. Dent Mater 2017;6:575-84

11. Puebla K, Arcaute K, Quintana R, Wicker RB. Effects of environmental conditions, aging, and build orientations on the mechanical properties of ASTM type 1 specimens manufactured via stereolithography. Rapid Prototyp J 2012;18:374-88

12. Unkoskiy A, Bui PH, Schille C, Geis-Gerstofer J, Huettig F, Spintzyk S. Objects build orientation, positioning, and curing influence dimensional accuracy and flexural properties of stereolithography printed resin. Dent Mater 2018;34:324-33.

13. Pfaffinger M, Hartmann M, Schwentenwein M, Stampfl J. Stabilization of tricalcium phosphate slurries against sedimentation for stereolithographic additive manufacturing and influence on the final mechanical properties. Int J App Ceram Tec 2017;4:499-506.

14. Anstis GR, Chantikul P, Lawn BR, Marshall DB. A critical evaluation of indentation techniques for measuring fracture toughness: I, direct crack measurements. J Eur Ceram Soc1981;9:533-8.

15. Tricoteaux A, Rguiti E, Chicot D, Boilet L, Descamps M, Leriche A, et al. Influence of porosity on the mechanical properties of microporous β-TCP bioceramics by usual and instrumented Vickers microindentation. J Eur Ceram Soc 2011;8:1361-9.

16. Ben Ghorbal G, Tricoteaux A, Thuault A, Louis G, Chicot D. Comparison of conventional Knoop and Vickers hardness of ceramic materials. J Eur Ceram Soc 2017;37:2531-5.

17. Domingues N, Galvão B, Ribeiro S, Junior A, Longhini D, Adabo G. Comparison of the indentation strength and single-edge-v-notched beam methods for dental ceramic fracture toughness testing. Braz J Oral Sci 2016;15:109-12.

18. International Organization for Standardization. ISO 14705:2016. Fine ceramics (advanced ceramics, advanced technical ceramics) - test method for hardness of monolithic ceramics at

room temperature. Geneva: International Organization for Standardization; 2016. AFNOR Store Order: N20200117-438973-T (Date: 2020-01-17). Available at: http://www.boutique.afnor.org.

19. ASTM STP678-EB. Fracture mechanics applied to brittle materials (Freiman 1979). West Conshohocken: ASTM, 1979:103-11.

20. Braga RR, Ballester RY, Ferracane JL. Factors involved in the development of polymerization shrinkage stress in resin-composites: a systematic review. Dent Mater 2005;21:962-70.

21. Suzuki TS, Uchikoshi T, Sakka Y. Control of texture in alumina by colloidal processing in a strong magnetic field. Sci Technol Adv Mat 2006;7:356-64.

22. Quinn JB, Quinn GD. A practical and systematic review of Weibull statistics for reporting strengths of dental materials. Dent Mater 2010;26:135-47.

23. Guazzato M, Albakry M, Ringer SP, Swain MV. Strength, fracture toughness and microstructure of a selection of all-ceramic materials. Part II. Zirconia-based dental ceramics. Dent Mater 2004;20: 449-56.

24. Uçar Y, Aysan Meriç I, Ekren O. Layered manufacturing of dental ceramics: fracture mechanics, microstructure, and elemental composition of lithography-sintered ceramic. J Prosthodont 2018;11:1-9

25. Sakar-Deliormanli A, Güden M. Microhardness and fracture toughness of dental materials by indentation method. J Biomed Mater Res B Appl Biomater 2006;76:257-64.

Corresponding author

Dr Marion Dehurtevent

Department of Prosthodontics

Faculty of Dentistry

University of Lille

FRANCE

Email: marion.dehurtevent@univ-lille.fr

TABLES

Table 1. Physical properties of 3 orientations (ZX, ZY, and XY) of SLA-manufactured ceramics

Evaluated parameter		**ZX-oriented specimen**	**ZY-oriented specimen**	**XY-orient**
Minimum resting period of slurry between polymerization of 2 layers (s) [no. of layers[*]; general manufacturing time (min)[**]]		7 [480[*]; 186[**]]	8 [86[*]; 47[**]]	11 [34[*]; 35
Density (%)		98.0 ± 0.4[a]	98.1 ± 0.4[a]	97.8 ± 0.7[a]
σ (MPa)		313.8 ± 27.9[b]	409.7 ± 29.6[c]	334.3 ± 62.
m [CI range 95%]		13.7 [12.4-15.1]	16.1 [14.6-17.5]	06.2 [05.6-
Hardness (GPa)	Length-width face	19.0 ± 2.5[d]	19.9 ± 1.6[d]	18.9 ± 2.1[d]
	Thickness-length face	19.0 ± 2.5[e]	19.7 ± 2.2[e]	20.1 ±2.4[e]
	Width-thickness face	19.6 ± 2.0[f]	19.9 ± 2.8[f]	20.5 ± 2.4[f]
K_1C by single-edge notch – 3-point flexural strength (MPa.m$^{1/2}$)		3.2 ± 0.2[g]	4.6 ± 0.2[h]	4.1 ± 0.1[gh]
K_1C by indentation (MPa.m$^{1/2}$)	Length-width face	3.1 ± 1.2[i]	4.9 ± 0.7[i]	4.2 ± 0.9[i]
	Thickness-length face	5.0 ± 1.3[j]	4.3 ± 1.7[j]	4.0 ± 1.7[j]
	Width-thickness face	3.9 ± 2.5[k]	4.6 ± 2.7[k]	2.5 ± 1.9[k]

σ, 3-point flexural strength; m, Weibull modulus; K_1C, fracture toughness. Different superscript letters indicate statistical differences b

FIGURES

Figure 1. A, Specifications and design of specimens. B, Design of rectangular parallelepipedic specimens with 3 orientations (ZX, ZY, and XY). Specimen faces named for further analysis (dark grey face: length-width; light grey face: thickness-length; white face: width-thickness). White lines: successive layers; black triangles: supporting pillars.

Figure 2. Boxplots (box: median, Q1, Q3; whiskers: 10-90 percentile) of 3 orientations (ZX, ZY, and XY) of SLA alumina ceramics. A, Density, B, 3-point flexural strengths. C, Fracture toughness by SEVNB. D, Vickers hardness of length-width face of SLA alumina ceramics. E, Vickers hardness of 3 orientations (ZX, ZY, and XY) of thickness-length face. F, Vickers hardness of 3 orientations (ZX, ZY, and XY) of width-thickness face. G, Fracture toughness by indentation of 3 orientations (ZX, ZY, and XY) of length-width face of SLA alumina ceramics. H, Fracture toughness by indentation of 3 orientations (ZX, ZY, and XY) of thickness-length face. I, Fracture toughness by indentation of 3 orientations (ZX, ZY, and XY) of width-thickness face. Different superscript letters indicate statistical differences between groups ($P<.05$).

Figure 3: Weibull plot comparing strength distribution of SLA alumina ceramics in 4 orientations (ZX, ZY, and XY). ZX- and ZY-oriented specimens had highest Weibull moduli (slope of linear regression line of set of points), with high degree of homogeneity and smaller variations in flexural strength.

Figure 4: Micrographs of 3 faces of ZX-, ZY-, and XY-oriented SLA alumina specimens (original magnification ×2000): length-width (dark grey face in Figure 1A, D, and G, respectively), thickness-length (white face in Figure 1B, E, and H, respectively), and width-thickness (light grey face in Figure 1C, F, and I, respectively) (black line=orientation of layer).

Figure 5. Micrographs of fracture surface after 3-point flexural testing of SLA alumina ceramic A, In ZX orientation. B, In ZY orientation. C, In XY orientation. *=transgranular fracture; original magnification ×1500.

Figure 6: Transposition of orientations of printed layers from specimens studied to complex crown framework shapes: ZX, XY, and ZY, A, C, and E in buccal view, B, D, and F in mesial view.

Figure 7. A, Recommended SLA orientations to manufacture complex frameworks (white bars: orientation of successive layers). B, Preparation of first right maxillary premolar for ceramic crown. C, SLA-manufactured alumina dental crown framework on first right maxillary premolar.

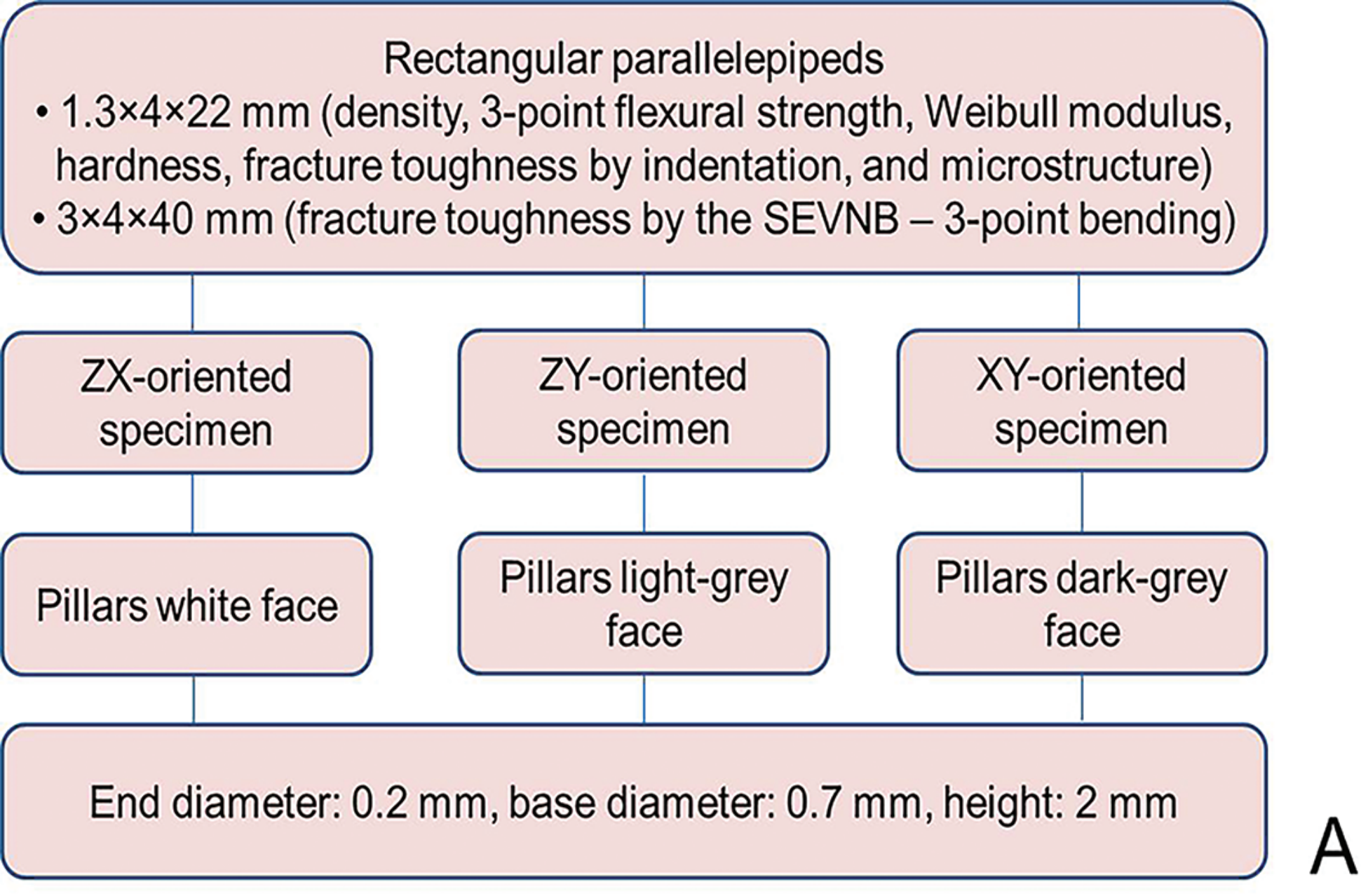
Rectangular parallelepipeds
• 1.3×4×22 mm (density, 3-point flexural strength, Weibull modulus, hardness, fracture toughness by indentation, and microstructure)
• 3×4×40 mm (fracture toughness by the SEVNB – 3-point bending)
ZX-oriented specimen
ZY-oriented specimen
XY-oriented specimen
Pillars white face
Pillars light-grey face
Pillars dark-grey face
End diameter: 0.2 mm, base diameter: 0.7 mm, height: 2 mm
A

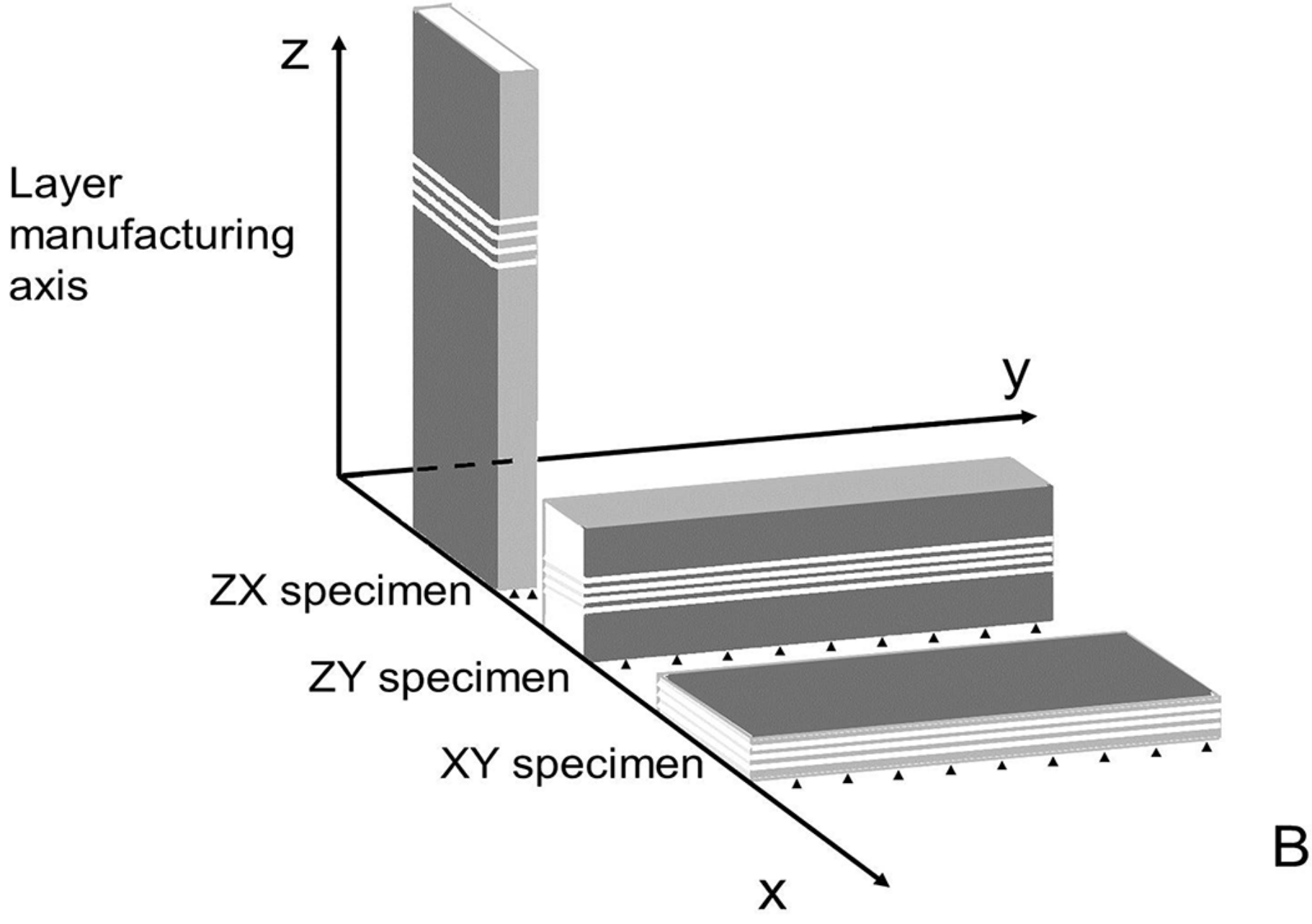
z
Layer
manufacturing
axis
y
ZX specimen
ZY specimen
XY specimen
x
B

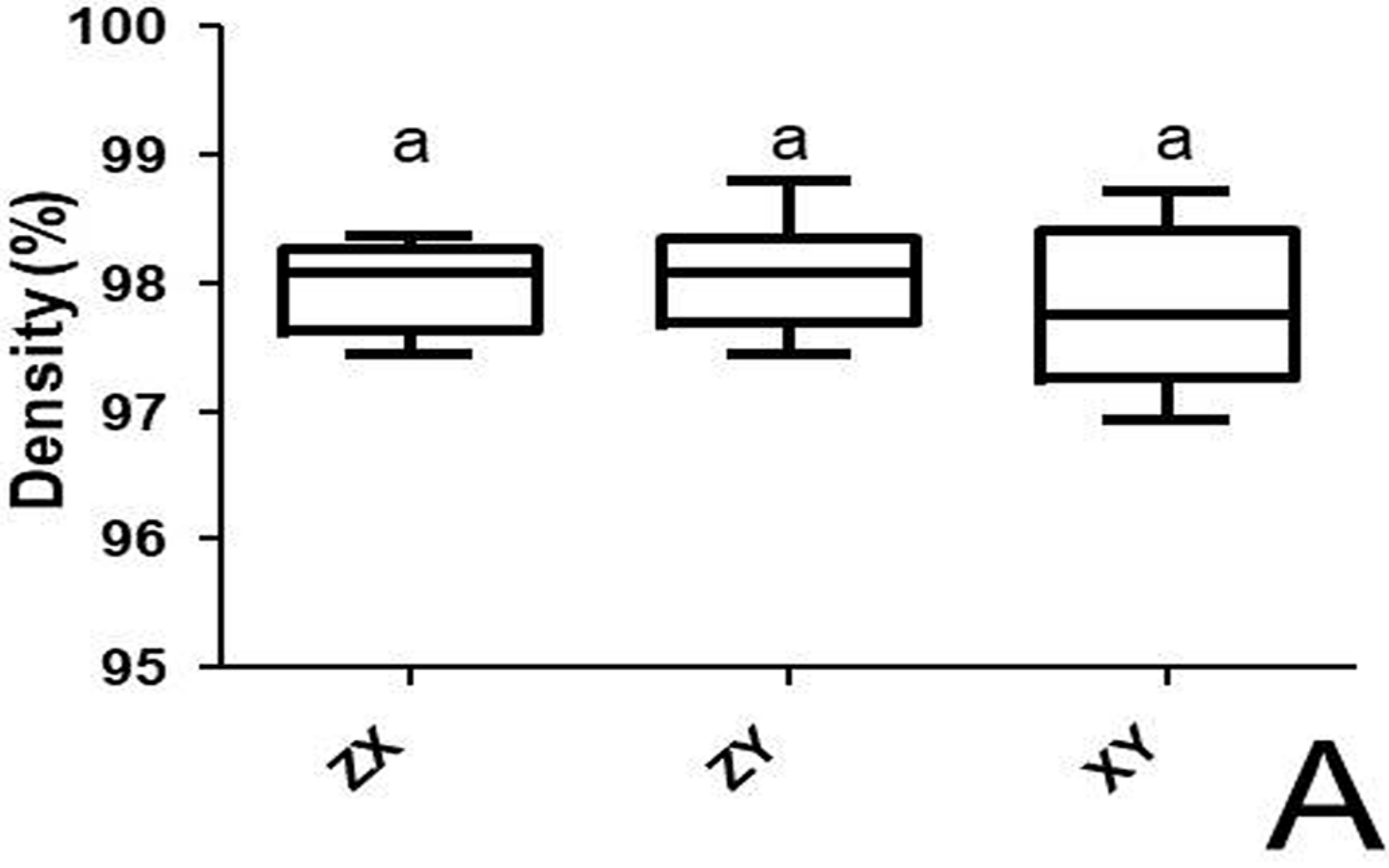
100
99
98
97
96
95
Density (%)
a
a
a
ZX
ZY
XY
A

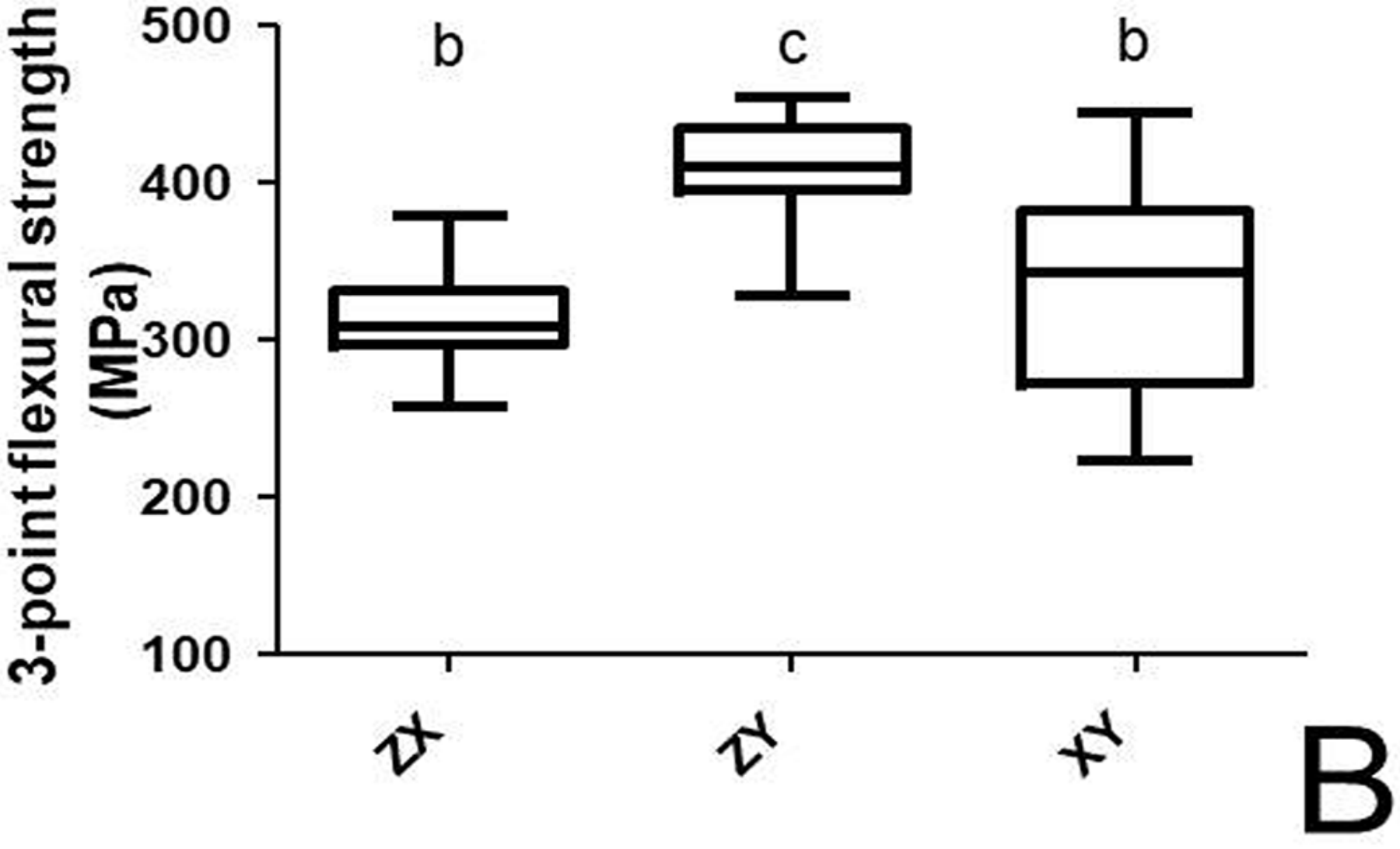
3-point flexural strength (MPa)
500
400
300
200
100
b
c
b
zx
zy
xy
B

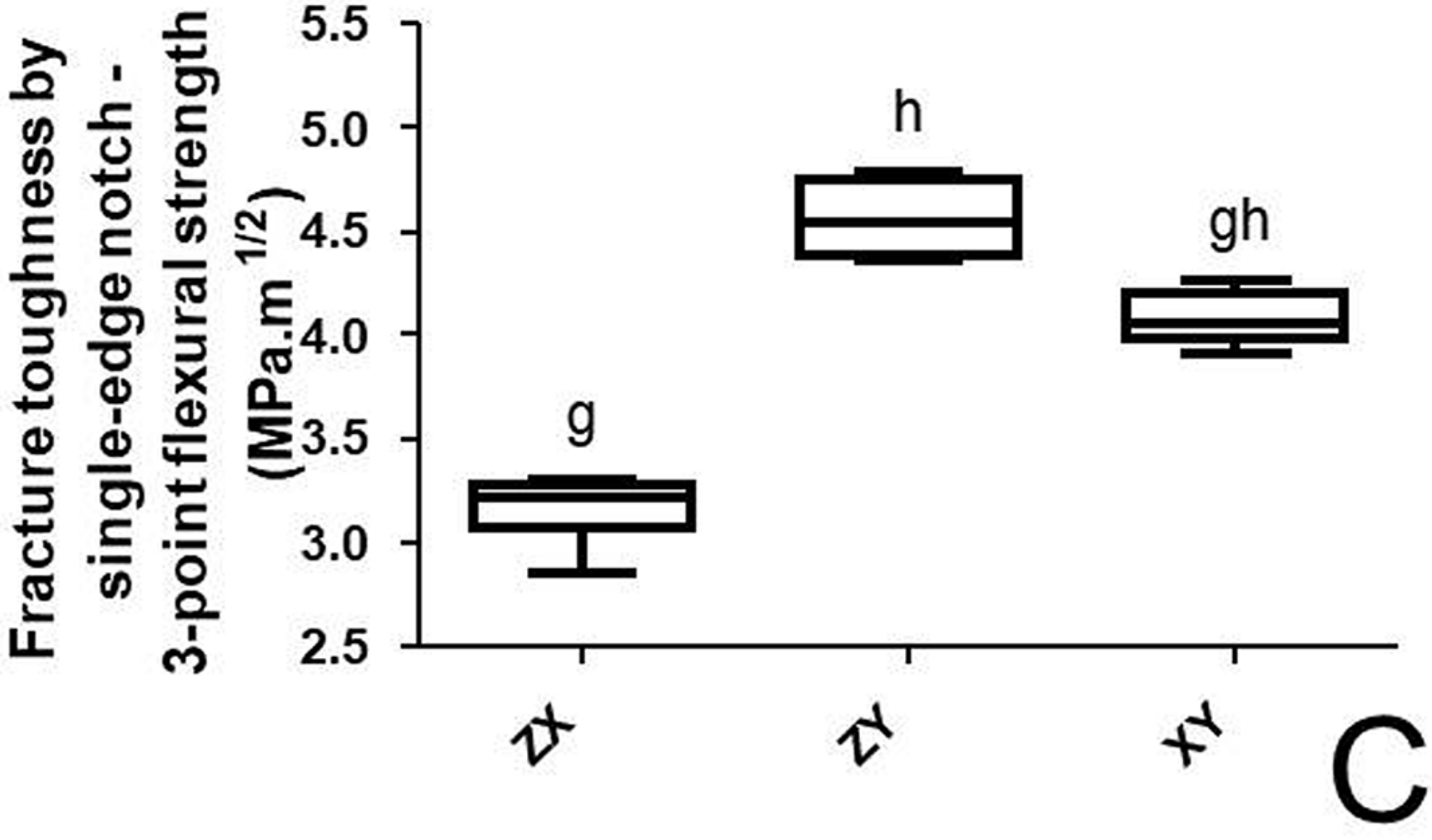
Fracture toughness by single-edge notch - 3-point flexural strength (MPa.m^1/2)
5.5
5.0
4.5
4.0
3.5
3.0
2.5
g
h
gh
zx
zy
xy
C

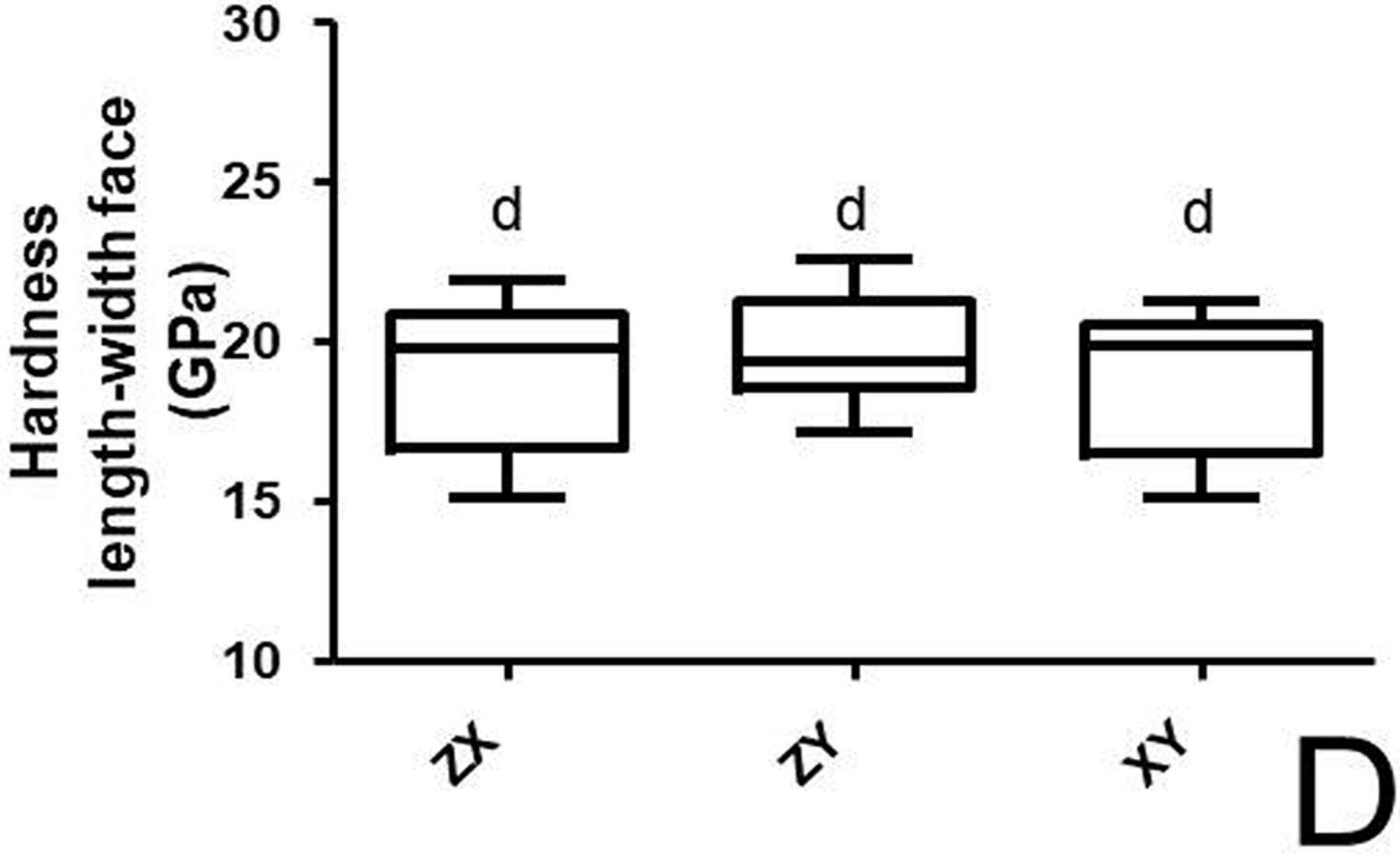
Hardness
length-width face
(GPa)
30
25
20
15
10
d
d
d
zx
zy
xy
D

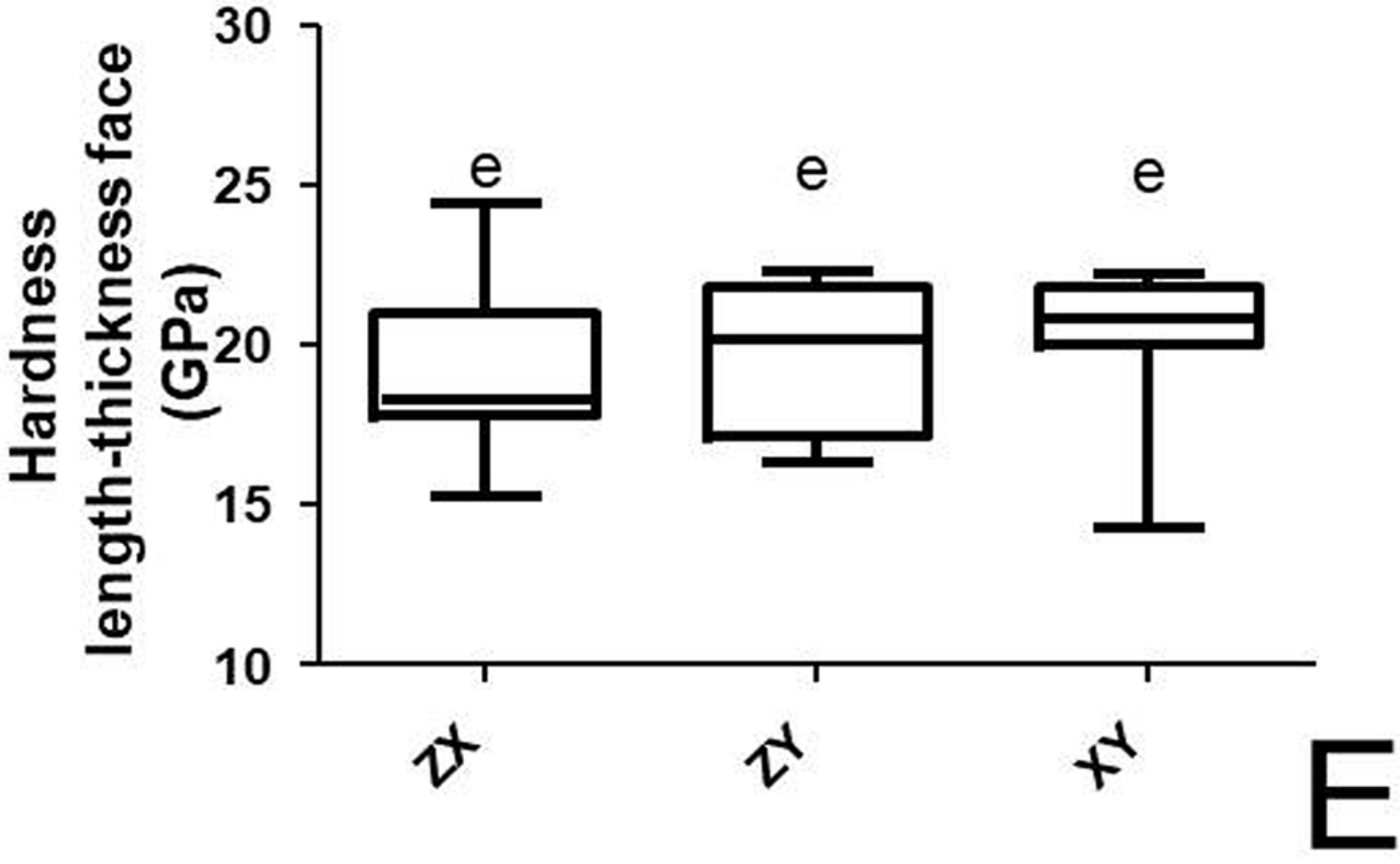
Hardness
length-thickness face
(GPa)
30
25
20
15
10
e
e
e
ZX
ZY
XY
E

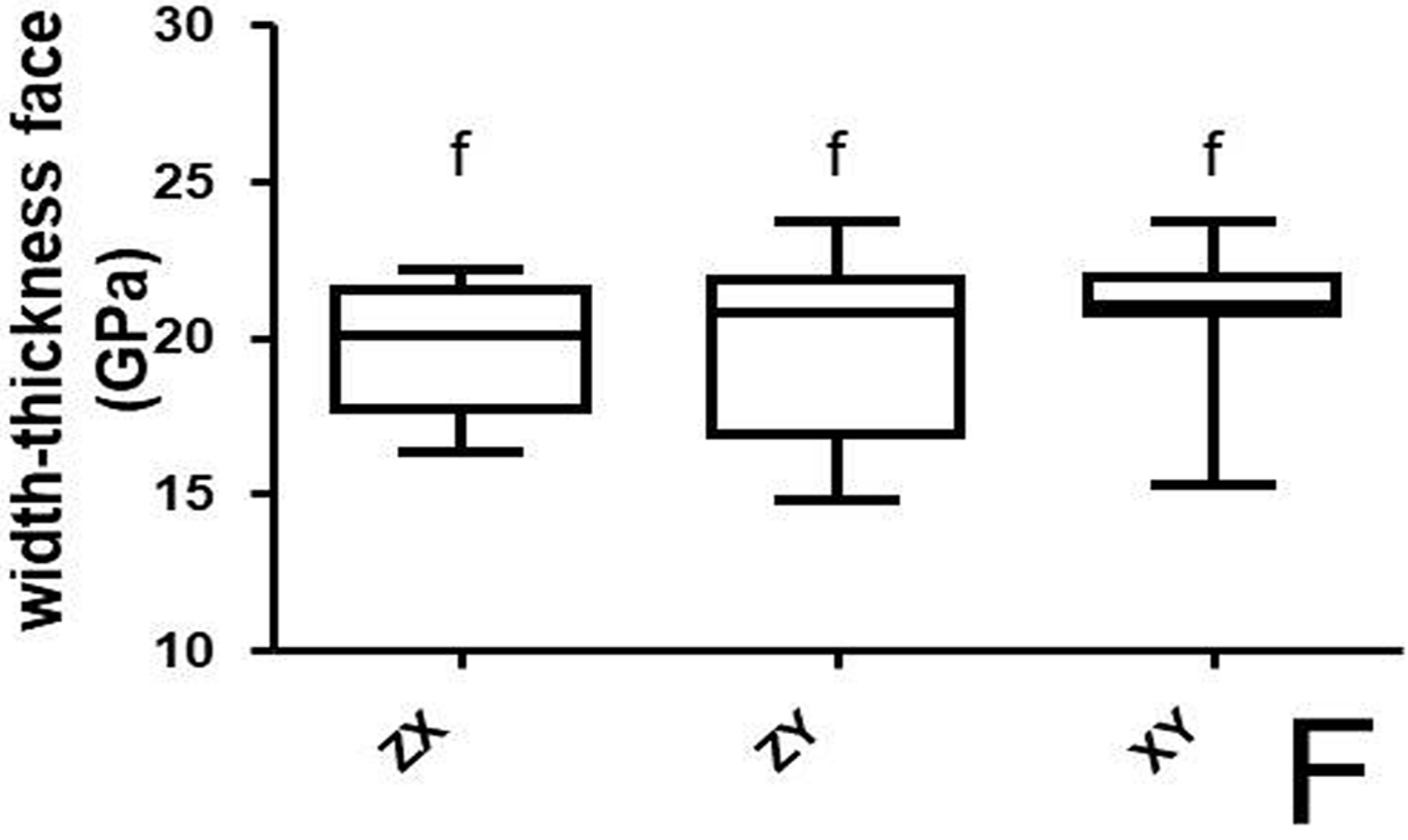
width-thickness face
(GPa)
30
25
20
15
10
f
f
f
ZX
ZY
XY
F

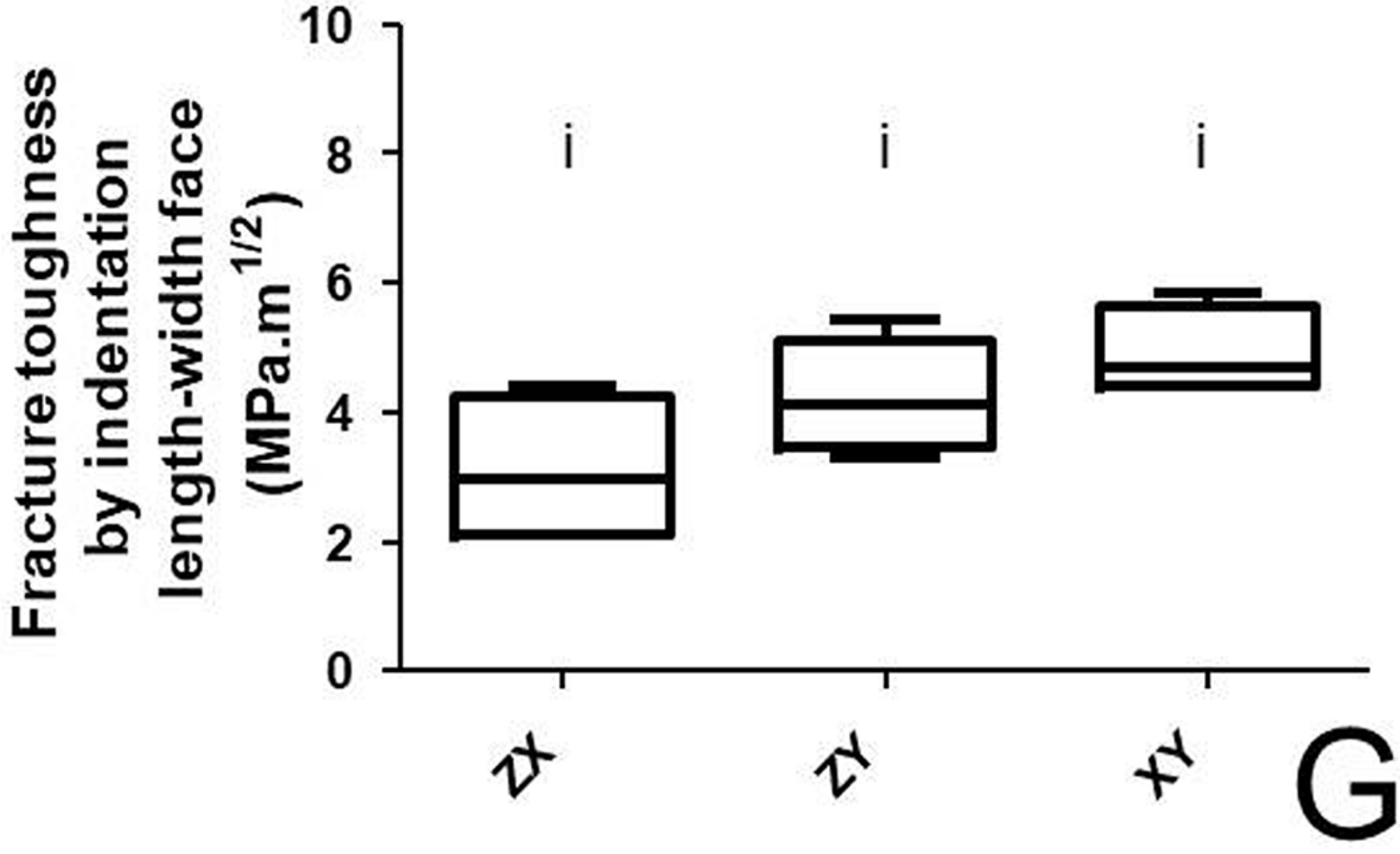
Fracture toughness
by indentation
length-width face
(MPa.m^1/2)
10
8
6
4
2
0
i
i
i
zx
zy
xy
G

Fracture toughness
by indentation
length-thickness face
(MPa.m 1/2)
0
2
4
6
8
j
j
j
zx
zy
xy

H

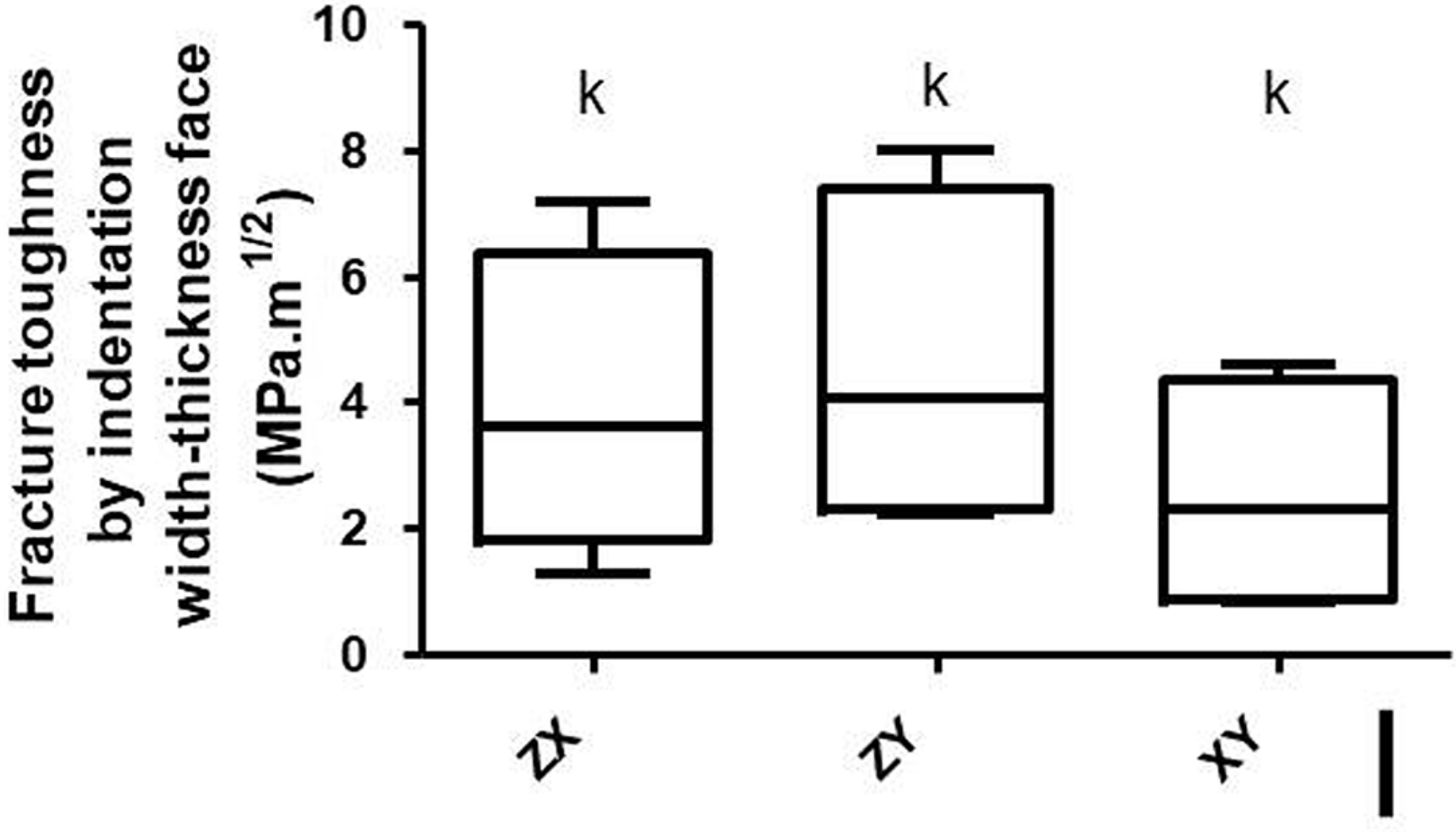
Fracture toughness
by indentation
width-thickness face
(MPa.m^1/2)
10
8
6
4
2
0
k
k
k
zx
zy
xy

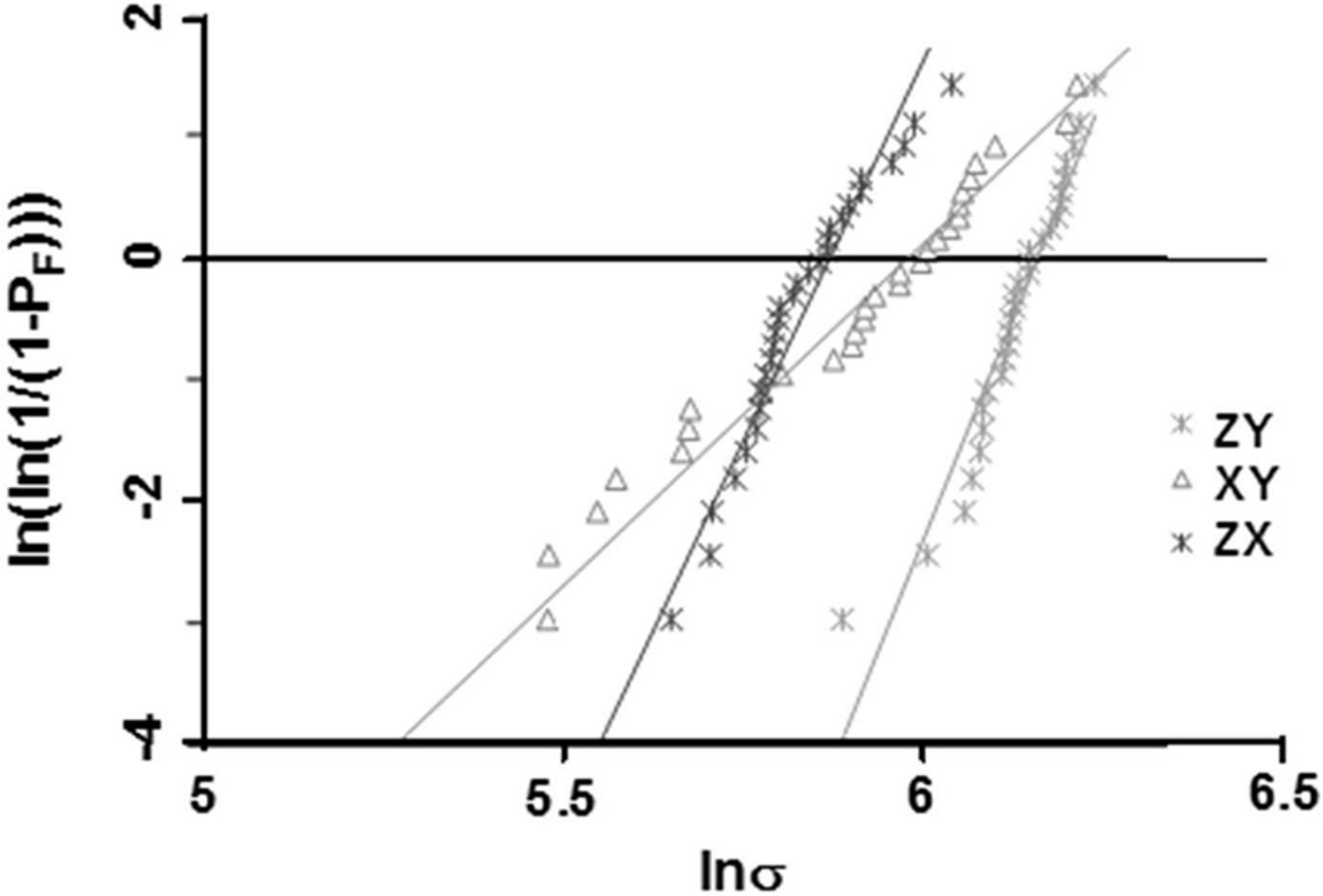
2
0
-2
-4
ln(ln(1/(1-P_F)))
5
5.5
6
6.5
lnσ
ZY
XY
ZX

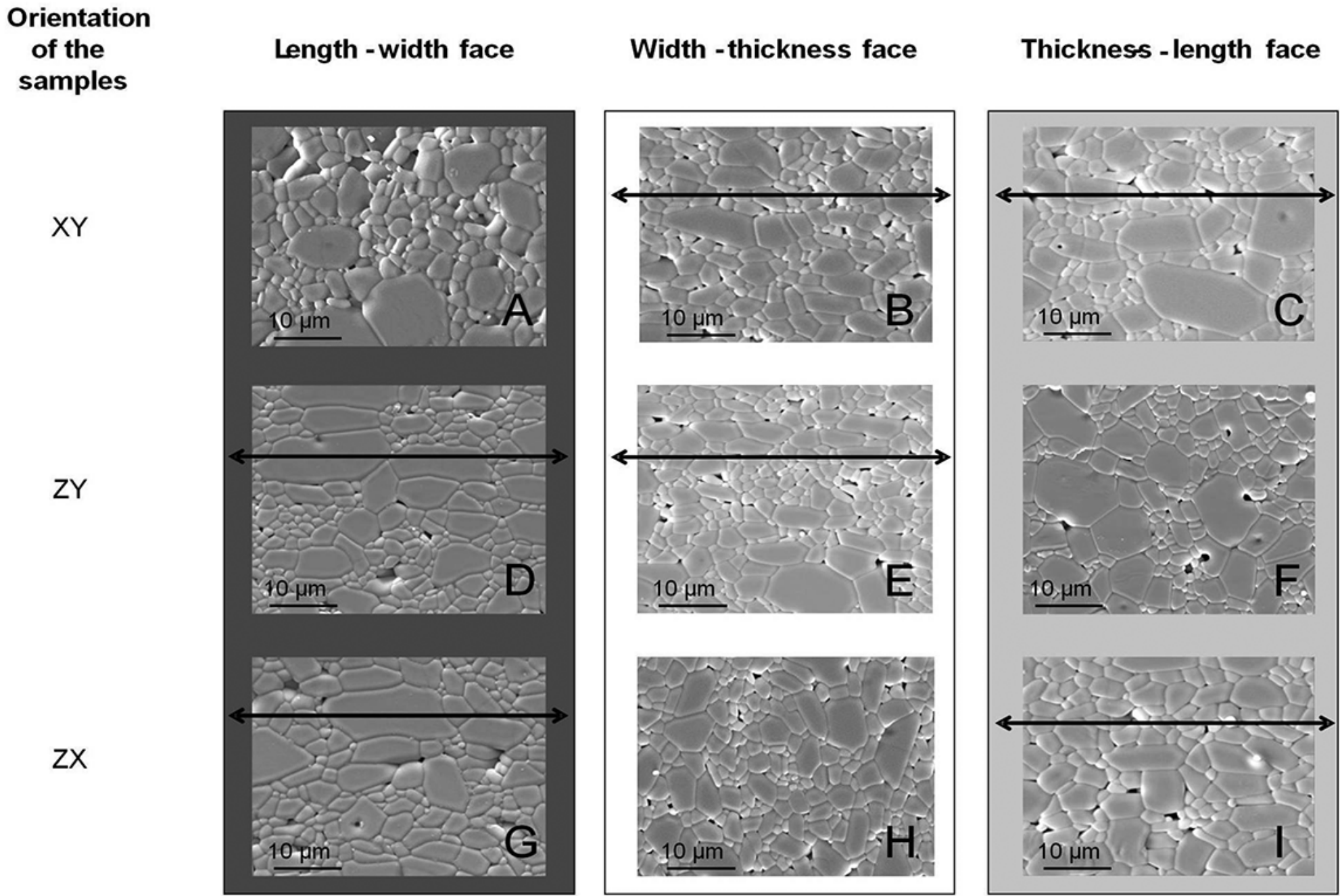
Orientation of the samples
Length - width face
Width - thickness face
Thickness - length face
XY
ZY
ZX
10 µm
A
B
C
D
E
F
G
H
I

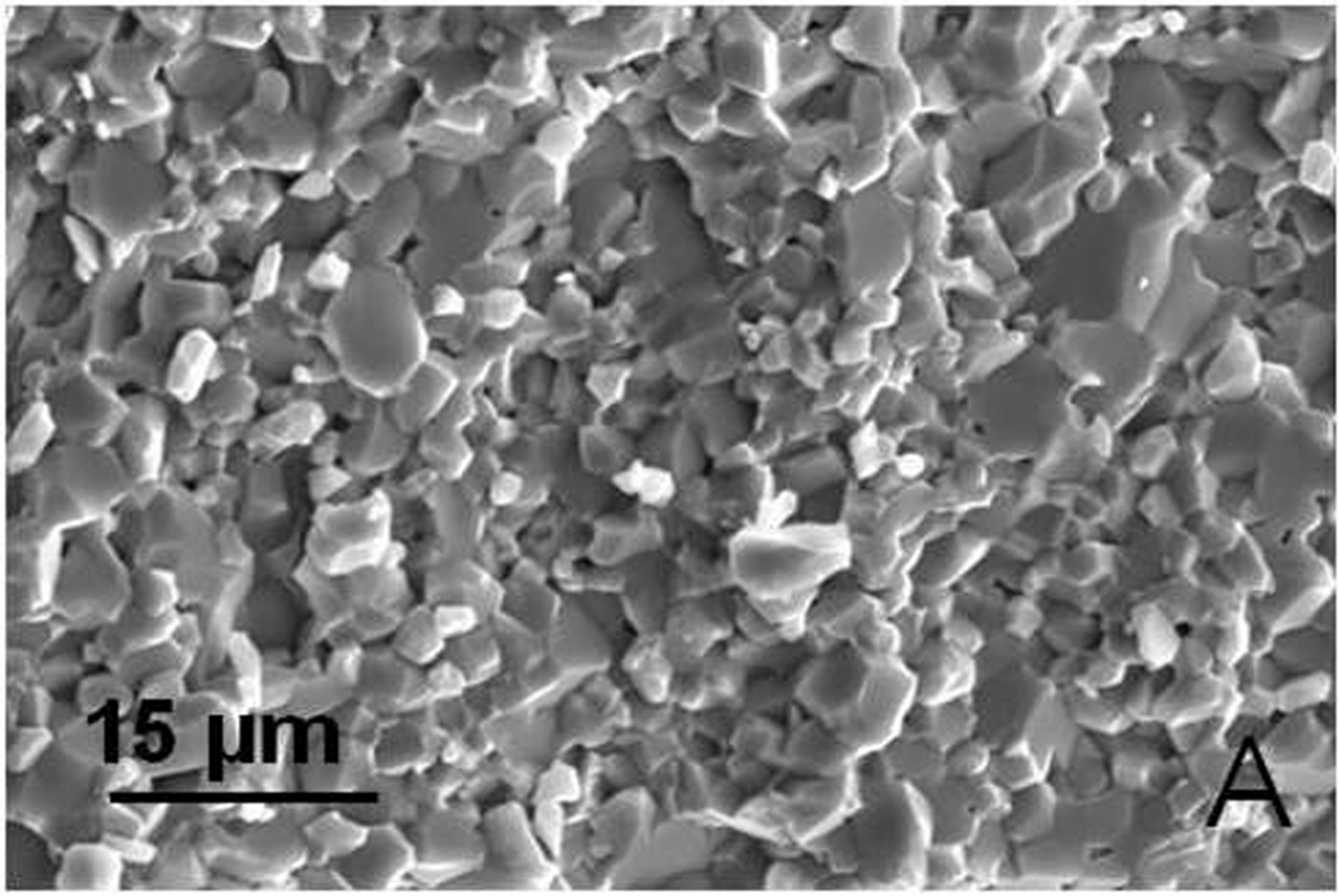
15 µm
A

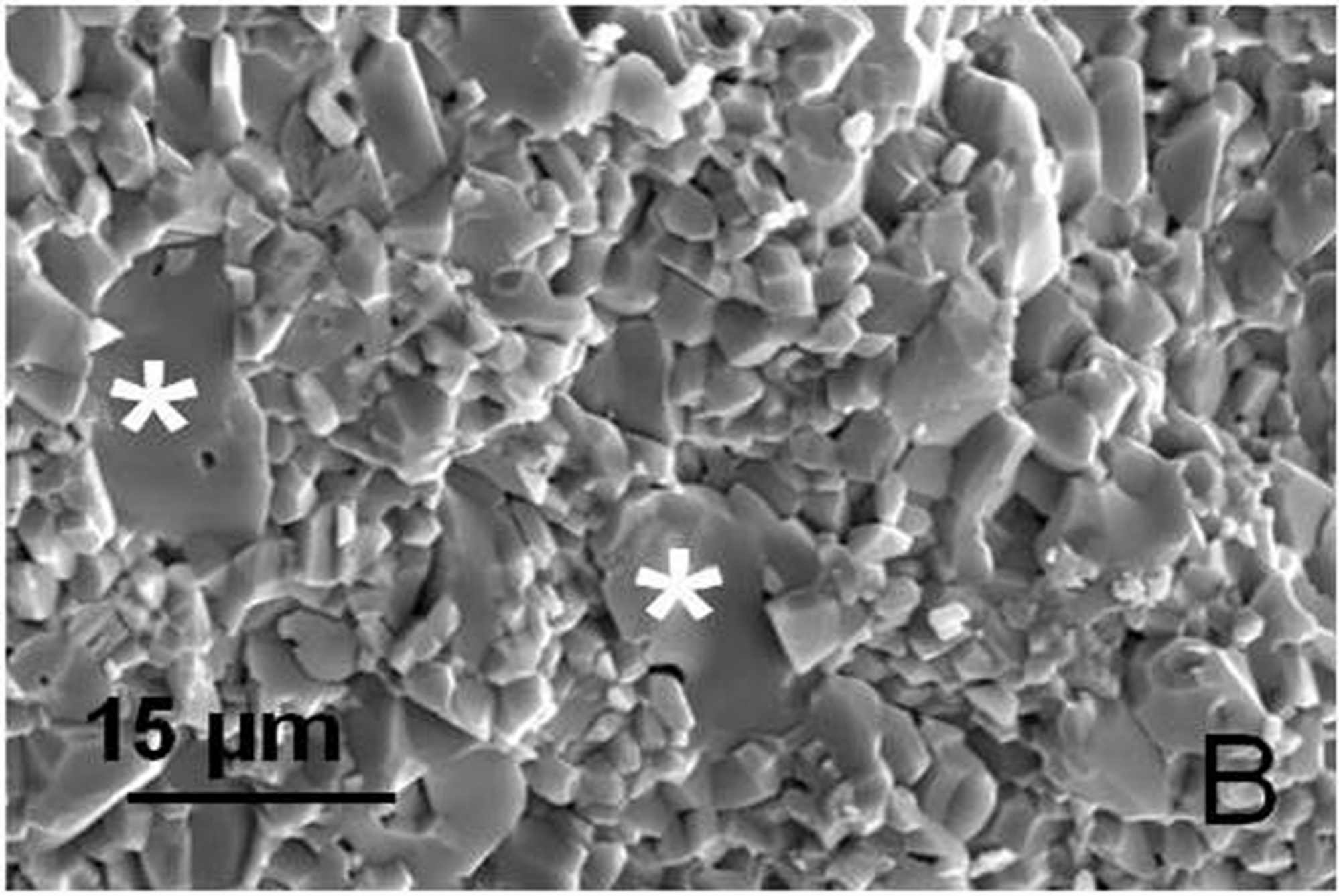
*
*
15 µm
B

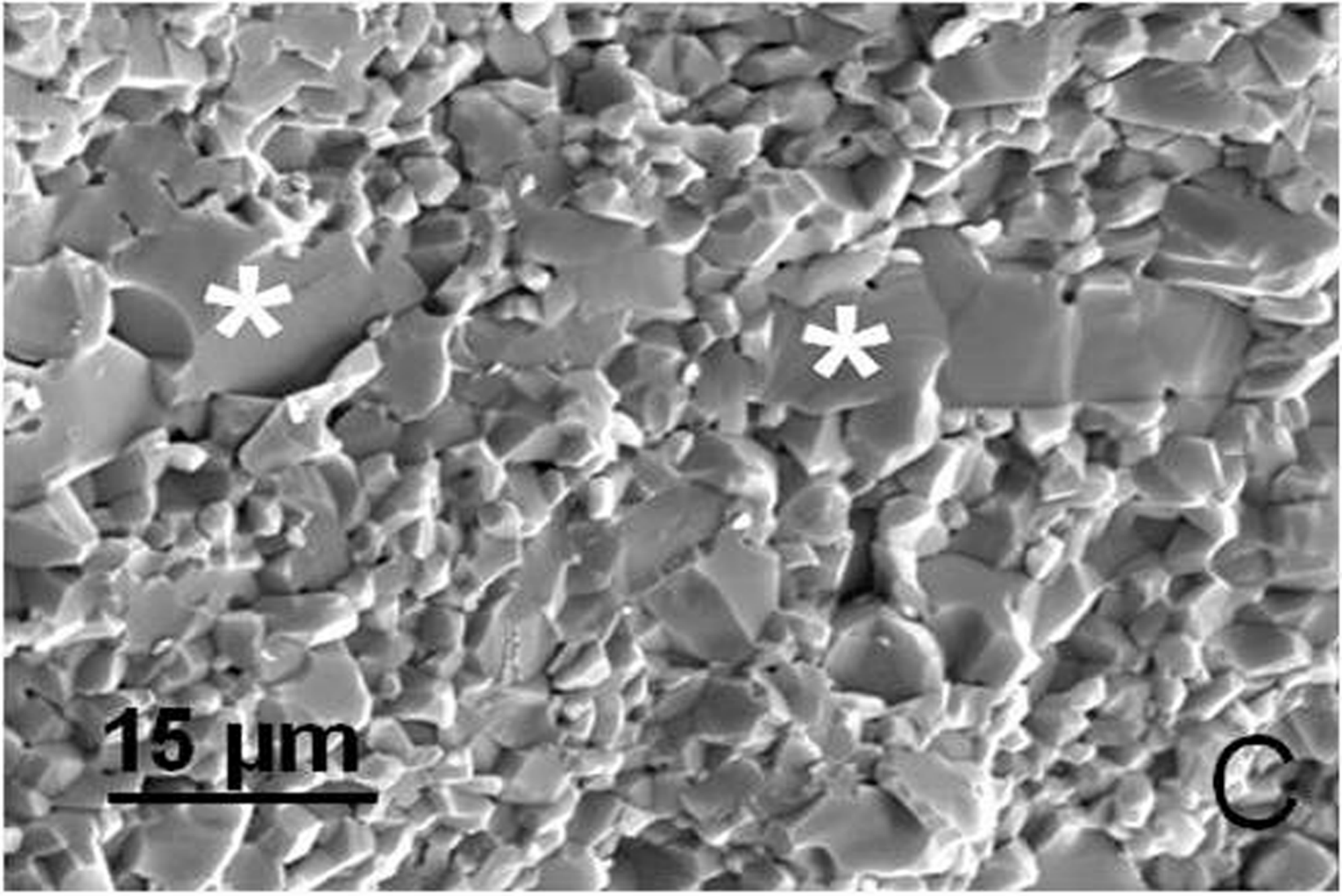
*
*
15 µm
C

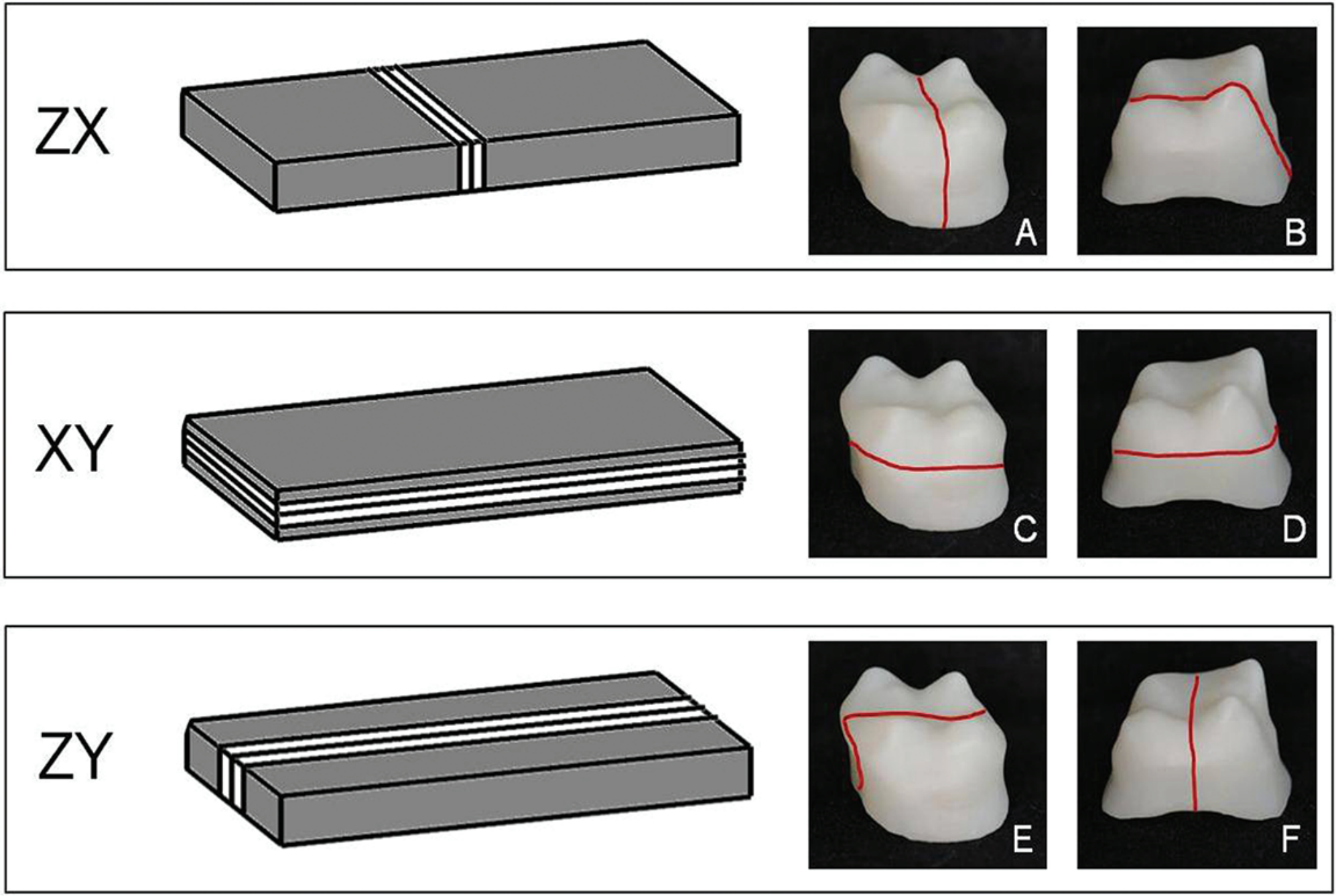
ZX
A
B
XY
C
D
ZY
E
F

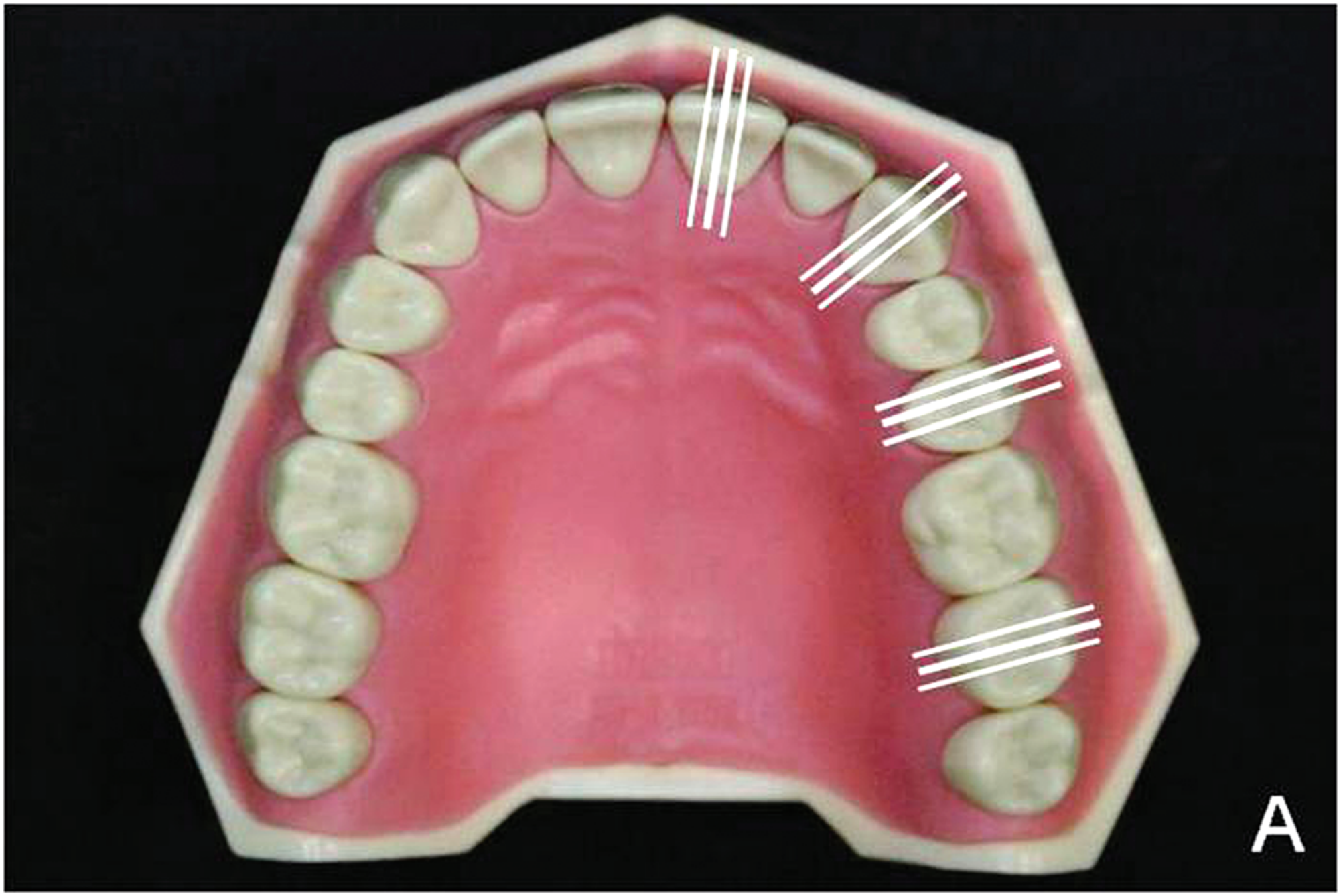
A

B

C

Evaluated parameter		**ZX-oriented specimen**	**ZY-oriented specimen**	**XY-oriented specimen**	***P***
Minimum resting period of slurry between polymerization of 2 layers (s) [no. of layers*; general manufacturing time (min)**]		7 [480*; 186**]	8 [86*; 47**]	11 [34*; 35**]	
Density (%)		98.0 ± 0.4[a]	98.1 ± 0.4[a]	97.8 ± 0.7[a]	.752
σ (MPa)		313.8 ± 27.9[b]	409.7 ± 29.6[c]	334.3 ± 62.1[b]	<.001
m [CI range 95%]		13.7 [12.4-15.1]	16.1 [14.6-17.5]	06.2 [05.6-06.8]	
Hardness (GPa)	Length-width face	19.0 ± 2.5[d]	19.9 ± 1.6[d]	18.9 ± 2.1[d]	.494
	Thickness-length face	19.0 ± 2.5[e]	19.7 ± 2.2[e]	20.1 ±2.4[e]	.236
	Width-thickness face	19.6 ± 2.0[f]	19.9 ± 2.8[f]	20.5 ± 2.4[f]	.427
K_1C by single-edge notch – 3-point flexural strength (MPa.m$^{1/2}$)		3.2 ± 0.2[g]	4.6 ± 0.2[h]	4.1 ± 0.1[gh]	.001
K_1C by indentation (MPa.m$^{1/2}$)	Length-width face	3.1 ± 1.2[i]	4.9 ± 0.7[i]	4.2 ± 0.9[i]	.078
	Thickness-length face	5.0 ± 1.3[j]	4.3 ± 1.7[j]	4.0 ± 1.7[j]	.779
	Width-thickness face	3.9 ± 2.5[k]	4.6 ± 2.7[k]	2.5 ± 1.9[k]	.472

σ, 3-point flexural strength; *m*, Weibull modulus; K_1C, fracture toughness. Different superscript letters indicate statistical differences between groups (P<.05).